Image and Vision Computing 27 (2009) 756–770

Contents lists available at ScienceDirect

Image and Vision Computing

journal homepage: www.elsevier.com/locate/imavis

Automatic noise estimation in images using local statistics. Additive and multiplicative cases

Santiago Aja-Fernández *, Gonzalo Vegas-Sánchez-Ferrero, Marcos Martín-Fernández, Carlos Alberola-López

LPI, E.T.S. Ingenieros de Telecomunicación, Universidad de Valladolid, 47011 Valladolid, Spain

ARTICLE INFO

Article history:
Received 8 May 2007
Received in revised form 11 January 2008
Accepted 4 August 2008

Keywords:
Noise estimation
Mode
Restoration
Gaussian noise
Local statistics

ABSTRACT

In this paper, we focus on the problem of automatic noise parameter estimation for additive and multiplicative models and propose a simple and novel method to this end. Specifically we show that if the image to work with has a sufficiently great amount of low-variability areas (which turns out to be a typical feature in most images), the variance of noise (if additive) can be estimated as the mode of the distribution of local variances in the image and the coefficient of variation of noise (if multiplicative) can be estimated as the mode of the distribution of local estimates of the coefficient of variation. Additionally, a model for the sample variance distribution for an image plus noise is proposed and studied. Experiments show the goodness of the proposed method, specially in recursive or iterative filtering methods.

1. Introduction

Noise estimation is a task of paramount importance in most image restoration techniques. These techniques are usually based on a degradation model where a noise-dependent-parameter is to be estimated and it controls the amount of filtering to be executed. For instance, the Wiener filter (in any of its multiple versions [1]) is built on the assumption that the image is corrupted by additive random noise. Thus the parameter to be estimated is the noise power spectrum or the variance of noise. If a Lee's filter [2] for multiplicative noise is considered, then the coefficient of variation (CV) of noise (i.e. the ratio of the standard deviation and the mean) is the one needed. Regardless of the theoretical goodness of the different methods to restore an image, the key point is the estimation of such noise parameters.

Noise estimation techniques in the spatial domain have been classified as block based and filtering based methods [3]. The former deals with the local standard deviation of the image, which is calculated using $M \times N$ blocks. In the latter, the image is filtered by a low-pass filter and the noise is estimated using the standard deviation of the difference between the original and the filtered images. A number of involved variations based on these approaches have been reported, such as methods based on wavelets [4,5], singular-value-decomposition [6], fuzzy logic [7] or median absolute deviation [8]. Alternatively, fast and simple solutions have also been reported [1]; for instance, in order to estimate the variance of additive noise, the minimum or the average of the locally estimated variances are considered, even though it is known that the former underestimates while the latter overestimates the pursued value [9,10]. In other fields this problem has also been tackled; specifically, in the context of speech processing some methods have being developed for time-varying background noise estimation, as the ones analyzed by [11,12].

In this paper, we present a novel approach based on local sample statistics, specifically on the distribution of such statistics. We will show that noise parameters may be accurately estimated using the mode of the population of local estimations. The mode is a fairly good estimator of the variance (if additive noise) or the CV (if multiplicative) of noise when the image to work with has a sufficiently great amount of low-variability areas so as to make the local hypothesis of "constant plus noise" acceptable; fortunately, this is not too a restrictive hypothesis for many real world (untextured) images. We will also show that an accurate estimation of noise is even more important when dealing with iterative or recursive filtering schemes, in which the level of noise varies from one iteration to another.

The paper is organized as follows: In Section 2 the additive and multiplicative models of noise used in this paper are introduced. Section 3 discusses the theory of the approach, Section 4 presents results and compares the methodology to other estimation procedures. Conclusions are summarized in Section 5. Some appendices have been added to ease the paper readability.

* Corresponding author. Tel.: +34 983 423660; fax: +34 983 423667.
E-mail addresses: sanaja@tel.uva.es (S. Aja-Fernández), gvegsan@lpi.tel.uva.es (G. Vegas-Sánchez-Ferrero), marcma@tel.uva.es (M. Martín-Fernández), caralb@tel.uva.es (C. Alberola-López).

0262-8856/$ - see front matter © 2008 Elsevier B.V. All rights reserved.
doi:10.1016/j.imavis.2008.08.002

2. Noise models and estimation

In this paper we will focus on images degraded by either additive or multiplicative noise. For the former we will consider the following model

$$g_{i,j} = f_{i,j} + n_{i,j} \tag{1}$$

where $f_{i,j}$ is the intensity at pixel (i,j) in the original image, $g_{i,j}$ is the intensity at pixel (i,j) in the degraded image and $n_{i,j}$ is a Gaussian noise sequence with zero mean and $\mathrm{Var}(n_{i,j}) = \sigma_n^2$ constant throughout the image. Assuming that the noise and the original image are independent, the variance of the degraded image can be written [1]

$$\sigma^2_{g_{i,j}} = \sigma^2_{f_{i,j}} + \sigma_n^2 \tag{2}$$

being both $\sigma^2_{g_{i,j}}$ and $\sigma^2_{f_{i,j}}$ local variances.

For the multiplicative noise the following the model will be used

$$g_{i,j} = f_{ij} u_{ij} \tag{3}$$

where $u_{i,j}$ is the multiplicative noise with mean and variance constant throughout the image and respectively denoted by $E[u_{i,j}] = \bar{u}$ and $\mathrm{Var}(u_{i,j}) = \sigma_u^2$. The (square) coefficient of variation (CV) of noise will be

$$C_u^2 = \frac{\sigma_u^2}{\bar{u}^2} \tag{4}$$

and it is also constant throughout the image. The local (square) CV of the degraded image is then defined as

$$C^2_{i,j} = \frac{\sigma^2_{g_{ij}}}{\bar{g}^2_{ij}} \tag{5}$$

where $\bar{g}_{i,j}$ is the local mean of the degraded image. This equation can be rewritten as [13,14]

$$C^2_{i,j} = \frac{\sigma^2_{f_{ij}}}{\bar{f}^2_{ij}}(1 + C_u^2) + C_u^2 \tag{6}$$

According to Eq. (2), if at some region the equality $\sigma^2_{f_{ij}} = 0$ holds, i.e., the image is locally constant (plus noise), then it is clear that

$$\sigma^2_{g_{i,j}} = \sigma_n^2 \tag{7}$$

Therefore, within a uniform area (in terms of the signal content) the variance of the degraded image equals the variance of noise. The same reasoning can be applied to Eq. (6) for multiplicative noise, i.e., within a homogeneous area

$$C^2_{i,j} = C_u^2 \tag{8}$$

Although this reasoning is well-known, some consequences should be taken into account (we will now focus on the additive case; the reasoning for the multiplicative case is similar, by replacing the variance with the CV): specifically, according to the previous statement, one straightforward way to estimate σ_n^2 is to calculate the variance within homogeneous regions [15,16], where the variance of the original image is close to zero, so Eqs. (7) and (8) hold. This method has the drawback of requiring either some sort of automatic procedure or manual selection to detect these homogeneous regions. It is also highly sensitive to errors, outliers and inhomogeneities.

Alternatively, if estimations were totally accurate, and according to Eq. (2), then σ_n^2 should be

$$\hat{\sigma}_n^2 = \sigma^2_{\min} = \min_{ij}\{\sigma^2_{g_{ij}}\} \tag{9}$$

However, this estimate is, in practice, biased towards zero due to the sensitivity of the min operator to outliers and the real distribution of the local variance estimator itself; as a result it frequently underestimates the real value of σ_n^2. Some authors use the average instead

$$\hat{\sigma}_n^2 = \sigma^2_{\mathrm{ave}} = \frac{1}{N}\sum_{ij}\sigma^2_{g_{ij}} \tag{10}$$

(with N the number of points in the summation) but this method tends, conversely, to overestimate.

A walk-around has been proposed elsewhere [9], where some intermediate value is calculated by introducing a free parameter λ ranging within the interval (0,1). The estimator is then

$$\hat{\sigma}_n^2 = \lambda\sigma^2_{\min} + (1-\lambda)\sigma^2_{\mathrm{ave}}. \tag{11}$$

Another common noise estimator in video and speech processing is [4]

$$\hat{\sigma}_n = \sigma_{\mathrm{MAD}} = 1.4826 \times \mathrm{MAD}(y^H_{i,j}) \tag{12}$$

which assumes the noise standard deviation as proportional to the median absolute deviation (MAD) of the wavelet coefficients in the highest frequency subband, $y^H_{i,j}$. The MAD is defined (for some dataset g_i)

$$\mathrm{MAD} = \mathrm{median}_i(||g_i - \mathrm{median}_k(g_k)||)$$

In [8], the authors propose a similar estimator for the CV

$$\widehat{C_u^2} = \frac{1.4826}{\sqrt{2}} \times \mathrm{MAD}(\nabla \log g_{i,j}) \tag{13}$$

As it has been stated in the introduction, more complex methods have also been reported in order to estimate noise statistics. These methods are not only based on the local variance $\sigma^2_{g_{ij}}$ but on other parameters of the image. See for example [3,5–7,17,18]. In this paper a novel simple procedure is introduced.

3. Noise estimation

Our aim is to find a fast, simple and reliable method to estimate σ_n^2 when additive Gaussian Noise is considered or C_u^2 for the multiplicative case. Let us take a previous practical view of the problem of estimation. We will focus first on the case of additive noise. According to Eq. (2) the theoretical effect of adding Gaussian noise to an image is that its local variance increases an amount σ_n^2. In Fig. 1 we show the reference image that we will use for this experiment, and the same image with additive Gaussian noise with zero mean and $\sigma_n = 20$ (for an image in the range [0,255]).

The (normalized) distribution of the local variance of the image is estimated and shown in Fig. 2a. According to Eq. (2) one would expect that the distribution of the noise image were just this distribution shifted to the right an amount σ_n^2, as shown in Fig. 2b. As previously stated, the straightforward estimator would be the minimum of the distribution, as in Eq. (9). However, as the sampling estimation of the local variance is used, this estimator will also have a variance itself [19], and its distribution differs from that

(a) Original image (b) Noisy image

Fig. 1. Real image used for the experiments. (a) Original image (256 gray levels). (b) Image with Gaussian noise with 0 mean and $\sigma_n = 20$.

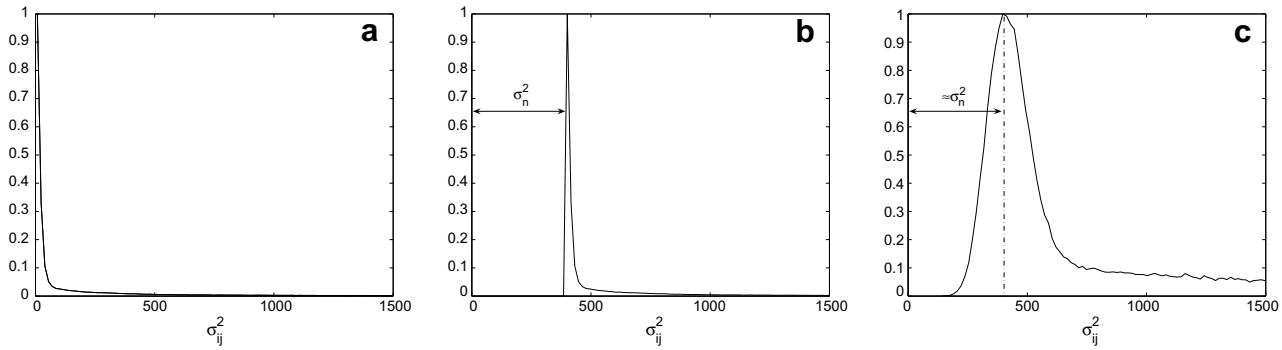

Fig. 2. Normalized (with respect to the maximum) distribution of local variance of the image. (a) Local variance distribution of the original image. (b) Theoretical variance distribution of the image with additive Gaussian noise. (c) Sample distribution of the sampling local variance of the image with additive Gaussian noise.

shown in Fig. 2b. Using a 7×7 window, the closer approximation to the distribution of the local variance in the noisy image is the one shown in Fig. 2c. As it is clearly shown in the figure, the mode of the distribution reflects the amount of noise. In the following section we will study this distribution assuming two different models. These assumptions will lead us to propose the mode as a good estimator for σ_n^2.

3.1. Sample variance in a Gaussian model

Let us first assume a simple Gaussian modeling of our problem. Let $X_i, i = \{1, \ldots, N\}$ be a set of random variables. If we accept that these variables correspond to the model *constant plus noise*, i.e., $X_i = a + W_i$, with $W_i, i = \{1, \ldots, N\}$, a set of independent and identically distributed (IID) Gaussian random variables with zero mean and standard deviation σ, the (unbiased) sampling variance is defined by

$$S^2 = \frac{1}{N-1}\sum_{i=1}^{N}(X_i - \overline{X})^2 \tag{14}$$

with

$$\overline{X} = \frac{1}{N}\sum_{i=1}^{N} X_i$$

the sample mean. The distribution of S^2 is well-known [19]; specifically, defining $Z = \frac{N-1}{\sigma^2}S^2$ then the probability density function (pdf) of Z is a chi-square with $N-1$ degrees of freedom ($Z \sim \chi^2_{N-1}$). Therefore

$$S^2 = \frac{\sigma^2}{N-1}Z \sim \gamma\left(x;\ \alpha = \frac{N-1}{2},\ \beta = 2\frac{\sigma^2}{N-1}\right) \tag{15}$$

with $\gamma(x;\ \alpha,\ \beta)$ the Gamma distribution [19], α the shape parameter and β the amplitude parameter, with pdf

$$p(x) = \gamma(x;\alpha,\beta) = \frac{1}{\Gamma(\alpha)}x^{\alpha-1}\left(\frac{1}{\beta}\right)^{\alpha}e^{-x/\beta}u(x) \tag{16}$$

being $u(x)$ the Heaviside step function.

The mean of S^2 turns out to equal the variance of noise, i.e.,

$$E\{S^2\} = \alpha\beta = \frac{N-1}{2}\frac{2\sigma^2}{N-1} = \sigma^2$$

If we replace the mean by its sample estimator then

$$\hat{\sigma}_n^2 = \frac{1}{N}\sum_{i,j}\sigma_{g_{i,j}}^2 \tag{17}$$

we obtain the maximum likelihood (ML) estimator of σ^2 for this model (see Appendix A.1).

Another possible estimator for this model could be the mode, which for the case that $\alpha > 1$ turns out to be $x_{\text{MODE}} = (\alpha-1)\beta$, and 0 otherwise [20]. Therefore, the mode of the sampling variance is (for $N > 2$)

$$\text{mode}\{S^2\} = \sigma^2\frac{N-3}{N-1} \tag{18}$$

which, for N moderately large, is fairly close to the value σ^2. So, an estimator of the variance of noise would be

$$\hat{\sigma}_n^2 = \frac{N-1}{N-3}\text{mode}\{\sigma_{g_{i,j}}^2\} \tag{19}$$

To make a preliminary test of the capability of estimation of the mode, an experiment is done. A 256×256 Gaussian image has been randomly generated, with mean 100 and $\sigma^2 = 400$. We have calculated the local variance using windows of size 3×3, 7×7, 11×11 and 31×31. The distribution of values are shown in Fig. 3. A correction of $\frac{N-1}{N-3}$ has been applied, being N the window size. The effect of changing the size of the window is a change in the width of the gamma-shaped distributions, but the maxima of those distributions are located at $\frac{N-3}{N-1}\sigma^2$. So, that maximum can be used to estimate σ^2, regardless of the size of the window used.

3.2. Sample variance in an image plus noise model

The assumptions of the previous section do not take into account the distribution of the local [signal] variance in the original image. Most of the images we usually deal with are images with a great amount of uniform areas. By *uniform area* we mean areas of the image without borders and with soft transitions. This means that, if no texture is present, the distribution of the local variances has its maximum value around zero.

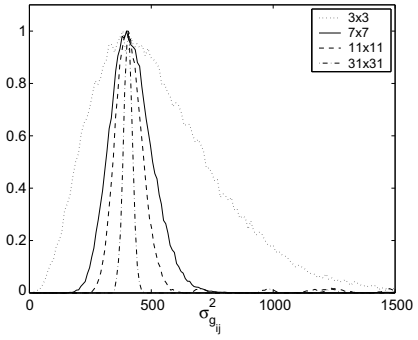

Fig. 3. Distribution of the sampling local variance, for different window size, normalized by $\frac{N-1}{N-3}$, being N the size of the window. Note that the mode is located on the same value, regardless of the value of N.

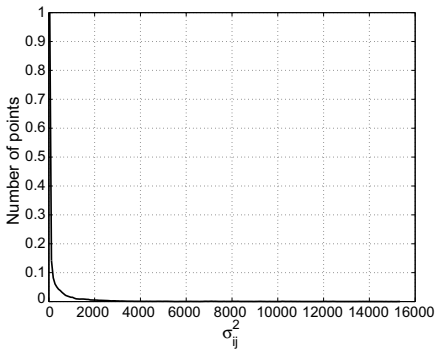

Fig. 4. (Normalized) Histogram of the values of the local variance in the image of Lenna.

To illustrate this statement, the distribution of the local variances in the Lenna image (see Fig. 11 left) with intensity values between 0 and 255 has been calculated, using 5×5 windows.[1] The result is depicted in Fig. 4, where it can be seen that most values are nearly zero, as expected. This exponentially decreasing histogram may be observed in a wide range of images, from natural scenes to medical images (see Appendix D). An obvious exception to this is the case of pictures of complex textures (see Section 4.3), for which intensity variability is considered signal content.

Assuming that the histogram of variances of an image with additive noise follows a Chi-Square distribution, as done in Section 3.1, involves leaving out the contribution of the signal to the final distribution. So, we need to take this into account in order to study its effect over the different estimators of noise.

This distribution is usually a decreasing function, but its actual shape will depend on the content of the image itself. Although it will not be possible to establish a universal model, some approximation can be made in order to study the behavior of the noisy image.

In Fig. 5 the estimated pdf of the Lenna image (Fig. 11 top-right) and the one of an MR image (Fig. 24) are depicted. The following models are considered:

1. Inverse function model:

$$p_f(x) = \begin{cases} \frac{(\beta_f - 1)K_f^{\beta_f - 1}}{(x+K_f)^{\beta_f}} u(x) & \beta_f > 1 \\ \frac{(\log(X_M/K_f+1))^{-1}}{(x+K_f)^{\beta_f}} u(x) & \beta_f = 1, \quad x \in [0, x_M] \end{cases} \tag{20}$$

2. Exponential model: Gamma distribution with the maximum in 0

$$p_f(x) \sim \gamma(x; 1, \beta_f) \tag{21}$$

being $\gamma(x; \alpha_i, \beta_i)$ the Gamma distribution, see Eq. (16).

The histogram for the Lenna image fits better a inverse function model with $\beta_f = 1$ (see Fig. 5a) while the MR image histogram fits better the exponential model with $\beta_f = 0.4$ (see Fig. 5b).

For the sake of simplicity and compactness of the solutions we will consider the local variance distribution of the original image to follow a Gamma distribution with the maximum in 0. Although this distribution may not totally fit the real data, it will illustrate how the variance of the original image affects the parameter estimation.

We denote $p_n(x)$ the distribution of local variances in a Gaussian noise image and $p_f(x)$ the distribution of local variances in a noise-free image.[2] According to Eq. (2), the variance of the image g will be the sum of the variances of image and noise. So, if they are modeled as independent random variables, the distribution of the sum will be the convolution [19]

$$p_g(x) = p_f(x) * p_n(x) = \gamma(x; 1, \beta_f) * \gamma(x; \alpha_n, \beta_n)$$

being $\alpha_n = \frac{N-1}{2}$ and $\beta_n = 2\frac{\sigma_n^2}{N-1}$, as defined in Section 3.1. We can write then

$$p_f(x) = \gamma(x; 1, \beta_f) = \left(\frac{1}{\beta_f}\right) e^{-x/\beta_f} u(x) \tag{22}$$

$$p_n(x) = \gamma(x; \alpha_n, \beta_n) = \frac{1}{\Gamma(\alpha_n)} x^{\alpha_n - 1} \left(\frac{1}{\beta_n}\right)^{\alpha_n} e^{-x/\beta_n} u(x) \tag{23}$$

and performing the convolution:

$$\begin{aligned} p_g(x) = p_f(x) * p_n(x) &= \int_0^x \frac{1}{\Gamma(\alpha_n)} t^{\alpha_n - 1} \left(\frac{1}{\beta_n}\right)^{\alpha_n} e^{-t/\beta_n} \left(\frac{1}{\beta_f}\right) e^{-(x-t)/\beta_f} dt \\ &= \frac{1}{\Gamma(\alpha_n)} \left(\frac{1}{\beta_n}\right)^{\alpha_n} \left(\frac{1}{\beta_f}\right) e^{-x/\beta_f} \int_0^x t^{\alpha_n - 1} e^{-t\left(\frac{1}{\beta_n} - \frac{1}{\beta_f}\right)} dt \\ &= \frac{1}{\Gamma(\alpha_n)} \left(\frac{1}{\beta_n}\right)^{\alpha_n} \left(\frac{1}{\beta_f}\right) e^{-x/\beta_f} \gamma_l\left(\alpha_n, \left(\frac{1}{\beta_n} - \frac{1}{\beta_f}\right)x\right) \left(\frac{1}{\beta_n} - \frac{1}{\beta_f}\right)^{-\alpha_n} \end{aligned}$$

being $\Gamma()$ the Gamma function and $\gamma_l()$ the lower incomplete Gamma function [21], which is defined as[3]

$$\gamma_l(a, x) = \int_0^x t^{a-1} e^{-t} dt \tag{24}$$

So, finally, the pdf of the noisy image will be

$$p_g(x) = \frac{1}{\Gamma(\alpha_n)} \frac{\beta_f^{\alpha_n - 1}}{(\beta_f - \beta_n)^{\alpha_n}} e^{-x/\beta_f} \gamma_l\left(\alpha_n, \left(\frac{1}{\beta_n} - \frac{1}{\beta_f}\right)x\right) u(x) \tag{25}$$

If $\beta_n = \beta_f$ the pdf is reduced to be a Gamma distribution with $\alpha_g = \alpha_n + 1$ and $\beta_g = \beta_n$.

Next step is to study how the inclusion of the signal model affects the noise estimators based on the mean and the model.

3.3. Mean of the distribution

As $p_g(x)$ is the distribution of the sum of two random variables, the mean of this distribution will be the sum of the mean of the distribution of each variable, $p_n(x)$ and $p_f(x)$:

$$E\{x\} = E_n\{x\} + E_f\{x\} = \alpha_n \beta_n + \beta_f$$

being $E_n\{x\}$ the mean of the distribution of the variance of noise and $E_f\{x\}$ the mean of the distribution of the variance of signal. We can rewrite it as

$$E\{\sigma^2_{g_{ij}}\} = \sigma_n^2 + E\{\sigma^2_{f_{ij}}\} \tag{26}$$

So, the variance of noise can be estimated as

$$\hat{\sigma}_n^2 = E\{\sigma^2_{g_{ij}}\} - E\{\sigma^2_{f_{ij}}\}$$

The ML estimator of σ_n^2 for this model turns out to be (see Appendix A.2):

$$(\widehat{\sigma_n^2})_{ML} = \left(\frac{1}{M}\sum_{i,j} \sigma^2_{g_{ij}}\right) - (\widehat{\beta_f})_{ML}$$

Thus, the reason why the average estimator (see Eq. (10)) tends to

[1] The size of the window is an important parameter as far as an estimation procedure is concerned. In [13] a comparative between estimation accuracy and window size is carried out.

[2] Note that in these two distributions x is the local variance.

[3] We will use the $\gamma_l()$ to denote the lower incomplete gamma function and $\gamma()$ to denote the Gamma distribution.

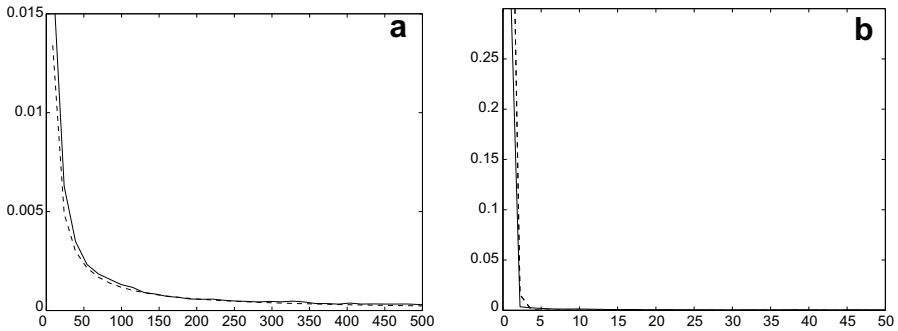

Fig. 5. Local variance distribution of images vs. models. (a) Distribution of variances in lenna image, see Fig. 11 (solid) vs. inverse function model (dashed) with $\beta_f = 1$ and $K_f = 0.2$. (b) Distribution of MR image, see Fig. 24 (solid), vs the exponential model (dashed) with $\beta_f = 0.4$.

overestimate is that the mean of the variance distribution of the noise-free image, i.e. $E\{\sigma^2_{f_{ij}}\}$ is not taken into account. The result is clearly a bias in the estimation. The simple Gaussian model usually employed is equivalent to consider the distribution of the local variances of the non-noisy image to be $p_f(x) = \delta(x)$, i.e, a constant image.

3.4. Mode of the distribution

In the case of the image plus noise model, the mode of the distribution in Eq. (25) is defined as

$$\text{mode}(p_g(x)) = \arg\max_x p_g(x)$$

Eq. (25) may be rewritten using an alternative expression for the lower incomplete Gamma function when α is an integer [21]

$$\gamma(\alpha_n, bx) = (\alpha_n - 1)!\left(1 - e^{-bx}\sum_{k=0}^{\alpha_n - 1}\frac{b^k x^k}{k!}\right)$$

with $b = \frac{1}{\beta_n} - \frac{1}{\beta_f}$. This way, Eq. (25) becomes

$$p_g(x) = \frac{(\alpha_n - 1)!}{\Gamma(\alpha_n)}\frac{\beta_f^{\alpha_n - 1}}{(\beta_f - \beta_n)^{\alpha_n}}e^{-x/\beta_f}\left(1 - e^{-bx}\sum_{k=0}^{\alpha_n - 1}\frac{b^k x^k}{k!}\right)u(x) \qquad (27)$$

To obtain the maximum we can leave all the constants aside and work with the following function

$$F_g(x) = e^{-x/\beta_f}\left(1 - e^{-bx}\sum_{k=0}^{\alpha_n - 1}\frac{b^k x^k}{k!}\right)u(x)$$
$$= \left(e^{-\frac{x}{\beta_n}\frac{\beta_n}{\beta_f}} - e^{-\frac{x}{\beta_n}}\sum_{k=0}^{\alpha_n - 1}\frac{\left(\frac{x}{\beta_n}\right)^k\left(1 - \frac{\beta_n}{\beta_f}\right)^k}{k!}\right)u(x)$$

Since

$$\arg\max_x p_g(x) = \arg\max_x F_g(x).$$

and making the change $y = x/\beta_n$

$$F_g(y) = \left(e^{-y\frac{\beta_n}{\beta_f}} - e^{-y}\sum_{k=0}^{\alpha_n - 1}\frac{y^k\left(1 - \frac{\beta_n}{\beta_f}\right)^k}{k!}\right)u(y)$$

The maximum of this function will depend on the values of α_n (related with N) and the ratio β_n/β_f. In Fig. 6 the argument of the maximum of function $F_g(y)$ is depicted for different values of the ratio β_n/β_f and α_n, normalized by the value $\alpha_n - 1$. In Fig. 7 the value is depicted for $\alpha_n = 24$ (corresponding to a 7×7 neighborhood) and for different values of β_n/β_f.

In Appendix B a complete study with an approximation is done. According to that study, if $bx \to 0$, (β_f and β_n are approximately of the same order)

$$\arg\max_x p_g(x) = \frac{\beta_f}{1 + b\beta_f}\alpha_n = \beta_n\alpha_n = \sigma_n^2$$

So, for this approximation

$$\hat{\sigma}_n^2 = \text{mode}(\sigma^2_{g_{ij}}). \qquad (28)$$

When the ratio β_n/β_f is small, it is equivalent to say that the image is *more variant* than the noise; which is the case when the noise level is low or the original image presents a highly variant pattern, as some textures. For $\beta_n \gg \beta_f$ (the opposite case) we can approximate

$$\arg\max_y(F_g(y)) \approx \alpha_n - 1$$

$$\arg\max_x(F_g(x)) \approx (\alpha_n - 1)\beta_n = \frac{N-3}{N-1}\sigma_n^2 \approx \sigma_n^2$$

The maximum of $F_g(x)$ is the maximum of $p_g(x)$. Therefore, the mode of the distribution may be approximated by

$$\text{mode}(p_g(x)) \approx (\alpha_n - 1)\beta_n = \frac{N-3}{N-1}\sigma_n^2 \approx \sigma_n^2$$

Note that when $\beta_f = \beta_n$ the mode is exactly σ_n^2, when $\beta_f/\beta_n > 2$ it is a very good approximation and for $\beta_f/\beta_n \in (0, 2]$ is a rough approximation, always based on the proposed model.

3.5. An intuitive point of view

As we have previously seen, most of the images that we usually deal with are images with a great amount of uniform areas, so the distribution of the local variances has its maximum value around zero. The distribution of the local variances in the Lenna image (Fig. 11 left) for instance, is shown in Fig. 4. The maximum of such distribution is placed in the origin, showing the an exponentially-shaped histogram that may be found in many images.

The distribution of the Lenna image with additive Gaussian noise ($\sigma_n^2 = 2000$) is now shown in Fig. 8a, and with $\sigma_n^2 = 700$ in Fig. 8b. As the variance of noise is constant throughout the picture it will affect every local variance value equally. As a result, the maximum of the bell-shaped distribution will reflect the local variance of the degraded image $g_{i,j}$ within homogeneous areas. This value is the mode of the distribution, and it is very close to the $\sigma_n^2, \text{mode}(\sigma^2_{g_{ij}}) \approx \sigma_n^2$ so we can use the mode to estimate it

$$\hat{\sigma}_n^2 = \text{mode}(\sigma^2_{g_{ij}})$$

The same reasoning can be applied to multiplicative noise. In this case, the distribution of the sampling local CV makes the analytical study more difficult. However, some conclusions can be drawn from experimental data, which will lead us to similar results as the ones obtained for additive noise. An analytical study of the pdf of this sampling CV may be found in Appendix C.

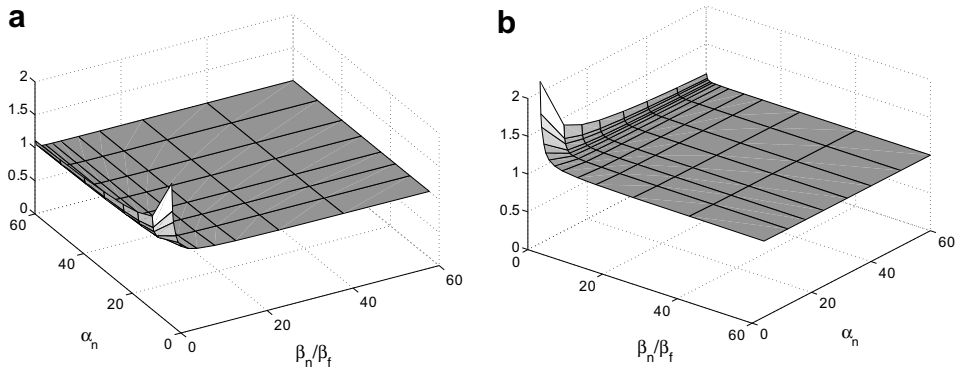

Fig. 6. Argument that maximizes the function $F_g(y)$ for different values of α_n and β_n/β_f, (normalized by $\alpha_n - 1$) two different views.

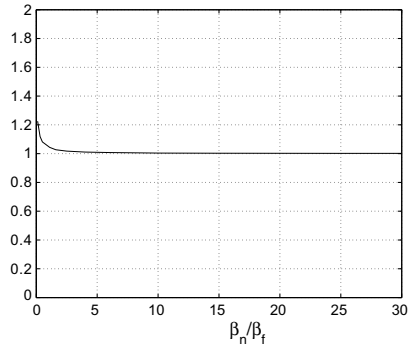

Fig. 7. Argument that maximizes the function $F_g(y)$ for $\alpha_n = 24$ $(N = 49)$ and different values of β_n/β_f, (normalized by $\alpha_n - 1$).

The distribution of the local CV for the Lenna image is shown in Fig. 9, and the distribution of the CV with multiplicative Gaussian noise (with $C_u^2 = 0.12$) in Fig. 10.

For this local statistic, we find again an exponential-like distribution with its maximum in zero. When the image is corrupted with multiplicative noise, the maximum is shifted nearby the value of the noise parameter to estimate, in this case, the CV

$$\hat{C}_u^2 = \text{mode}(C_{i,j}^2) \tag{29}$$

The problem of estimating the mode of a discrete population is a very well known problem in the statistics field, and it has been studied deeply in literature, see for instance [22,23]. It is beyond the scope of this paper to give a solution to this problem. If practical difficulties to properly estimate the mode arise, it may be useful to use the median operator instead, due to its greater simplicity and the fact that both parameters, albeit different, are not in practice far apart. So an alternative estimation procedure can be done by

$$\hat{\sigma}_n^2 = \text{median}(\sigma_{g_{i,j}}^2) \tag{30}$$

$$\hat{C}_u^2 = \text{median}(C_{i,j}^2) \tag{31}$$

Next section gives further insight by means of additional experiments.

4. Some experiments

4.1. Verification of the hypotheses

To further verify the hypotheses proposed in the previous section, some experiments have been carried out. First, we compare five different estimators for additive noise: average ($\hat{\sigma}_{\text{ave}}^2$), mini-

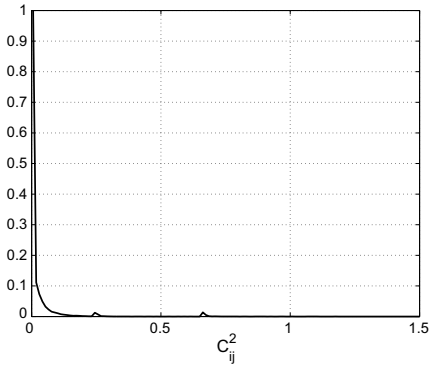

Fig. 9. Normalized histogram of the values of the local CV in the image of Lenna.

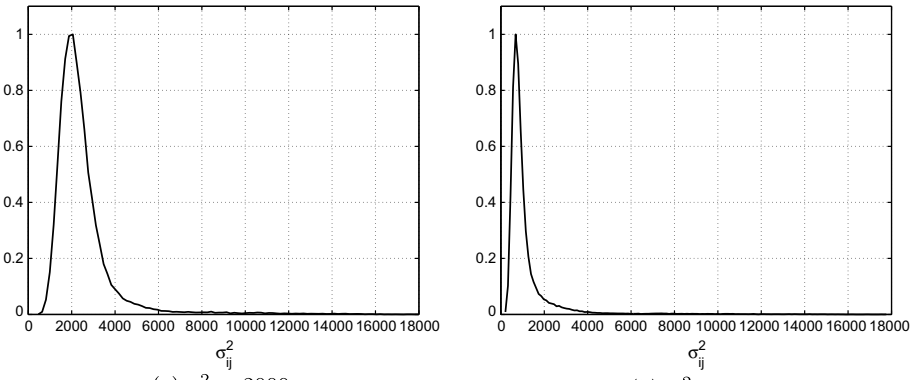

(a) $\sigma_n^2 = 2000$. (b) $\sigma_n^2 = 700$.

Fig. 8. Normalized histogram of the values of the local variance in the image of Lenna with Gaussian additive noise.

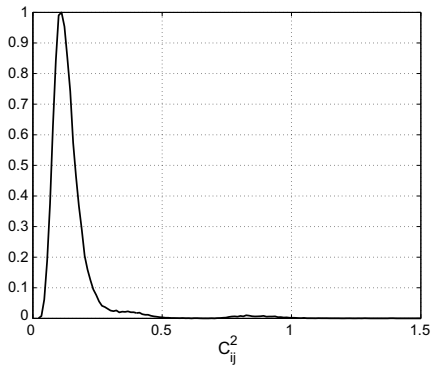

Fig. 10. Normalized histogram of the values of the local CV in the image of Lenna with multiplicative noise (Gaussian with $C_u^2 = 0.12$).

mum ($\hat{\sigma}^2_{\min}$), median absolute deviation ($\hat{\sigma}_{\mathrm{MAD}}$), median ($\hat{\sigma}^2_{\mathrm{med}}$) and mode ($\hat{\sigma}^2_{\mathrm{mod}}$). To that end, the three images in Fig. 11 with intensities between 0 and 255 are corrupted with additive Gaussian noise with different σ_n^2 values. Local variances are calculated within 7×7 windows. For each σ_n^2 the average value of 100 simulations over each image is computed. As a quality measure we will consider the relation $Q = \hat{\sigma}_{est}/\sigma_n$, being $\hat{\sigma}_{est}$ each of the five estimators. Clearly, the closer Q to 1 the better the estimator. Results are shown in Fig. 12.

It can be seen that the mode is the best among the estimators analyzed; it shows a better performance than the other methods for a wide range of variances, specially for small values. The median also shows a good performance except in the small-variance area. The MAD estimator shows a performance between the mode and the median.

As the variance increases, see Fig. 12b, it can be seen a convergence of the estimators, due to the fact that the data is closer to the pure Gaussian case, where mean, mode and median coincide. To assess these results, the experiment is done again using 29 images from the LIVE database [24] and averaging the results of another 100 experiment for each σ_n^2 value. Results are depicted in Fig. 13, with a similar performance to the previous experiment.

The experiment with the images in Fig. 11 is now repeated using multiplicative Gaussian noise with different C_u^2 values, see Fig. 14. The results for the mode and the median are similar to those of the additive case.

From these experiments it is noticeable that the mode is a good estimator and it presents a stable behavior for a wide range of values of the noise variance, including the smallest ones. We also want to point out the performance of the median estimator. Although it is not as accurate as the mode for small variances, its performance improves for larger values and it is easier to calculate.

Fig. 11. Original images used in the experiments.

4.2. Experiments of estimation and filtering

In this section we will show the performance of some well-known filters when noise estimation is carried out as proposed in the paper. We will begin with a 2D Wiener filter for additive noise and then we will deal with a Lee's filter for multiplicative models.

An adaptive Wiener filter [1,2] applied to the model given in Eq. (1) is defined as

$$\hat{f}_{i,j} = \bar{f}_{i,j} + \frac{\sigma^2_{f_{i,j}}}{\sigma^2_{f_{i,j}} + \sigma_n^2}(g_{i,j} - \bar{g}_{i,j}) \tag{32}$$

The Lenna image in Fig. 15a is corrupted with additive Gaussian noise with $\sigma_n = 25$, see Fig. 15b. Different operators will be used to estimate the variance of noise. The image will be filtered recursively 10 times. If noise power is estimated correctly, the filter should not degrade the image but eliminate the noise. If it is overestimated, there is a risk of blurring the image, and if underestimated, the noise will not be removed. The experiment results are on Fig. 15c–j. In order to make a quantitative comparison we have also calculated the measure of structural similarity for images (SSIM quality index [25]) on the course of 50 iterations, as shown in Fig. 16a. This measure is based on the adaptation of the human visual system to the structural information in a scene. The index accounts for three different similarity measures, namely, luminance, contrast and structure. The closer the index to unity, the better the result. Additionally, Fig. 17 shows a comparison of the histogram of local variances for the different estimators and the original image.

If the mode is used as the estimator of noise power, the filter cancels the noise out while blur is kept to a minimum. As previously stated, the average tends to overestimate; this may not be a critical problem when the noise variance is not small (as it may

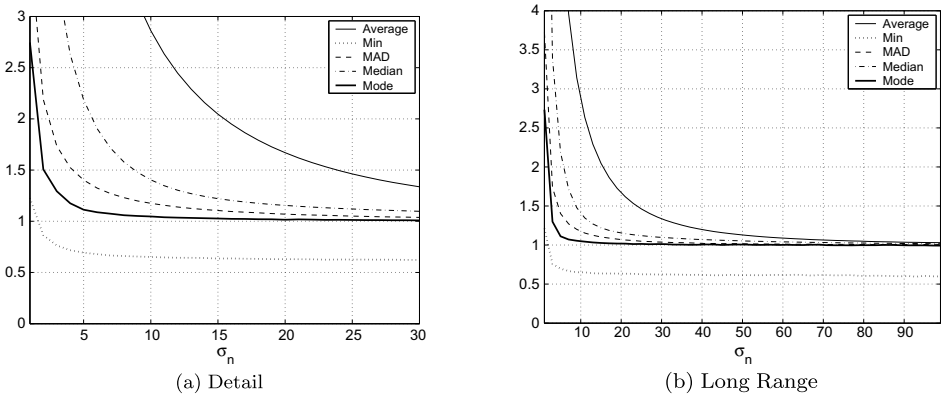

Fig. 12. Estimation of additive Gaussian noise for different values of σ_n. Quality measure $Q = \hat{\sigma}_{est}/\sigma_n$.

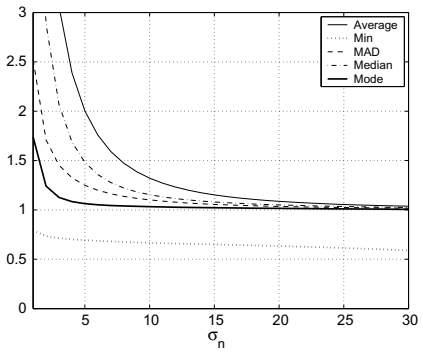

Fig. 13. Estimation of additive Gaussian noise for different values of σ_n using 29 images from the LIVE database. Quality measure $Q = \hat{\sigma}_{est}/\sigma_n$.

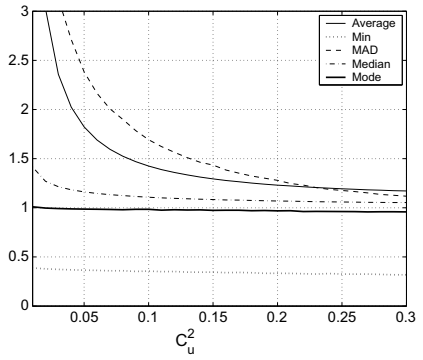

Fig. 14. Estimation of Gaussian multiplicative noise for different values of C_u^2. Quality measure $Q = (\widehat{C_u^2})_{est}/C_u^2$.

be the case in the first iteration), but when it decreases, the net result of this overestimation is a perceivable blur in the image, see Fig. 15d. On the other hand, the estimator based on MAD also shows a stable behavior for recursive filtering, as well as good SSIM values. Although MAD is a good estimator, the long term behavior of the mode-based estimator is slightly better.

As seen before, the performance improvement of the mode-based estimator is higher for smaller values of σ_n. To highlight this fact, the experiment has been done again with $\sigma_n = 7$. Results for the SSIM index are depicted in Fig. 16b. Again, this estimator is the one that shows the best results.

This example points out the importance of an estimator in recursive filters to have a good performance for different variances. As the variance decreases in every step, an overestimation in small values leads the recursive filter to draw undesired results.

A similar experiment is carried out for multiplicative noise. The image is now degraded with multiplicative Gaussian noise with $C_u^2 = 0.036$. The corrupted image is filtered using a Lee's filter for multiplicative noise [2]

$$\hat{\bar{u}}_{i,j} = \bar{g}_{i,j} + \frac{C_{i,j}^2 - C_u^2}{C_u^4 + C_{i,j}^2}(g_{i,j} - \bar{g}_{i,j}) \tag{33}$$

Results are shown in Figs. 18 and 19. As we are working with a small value of C_u^2, the average and median estimators show a very poor performance.

As we have previously said, in some cases it may be useful to use the median instead of the mode, due to the fact that the former is easier to calculate, and it is better estimator than the mean. However, as it has been shown in the experiments, it is not an appropriate choice when recursive filtering is carried out due to the over-estimation problem.

4.3. Limitations

If the assumption on which the paper is grounded is not held, the estimator based on the mode of the distribution of local variance (for additive noise) or of local CV (for the multiplicative case) is not worth taking. This is very easily checked by means of an

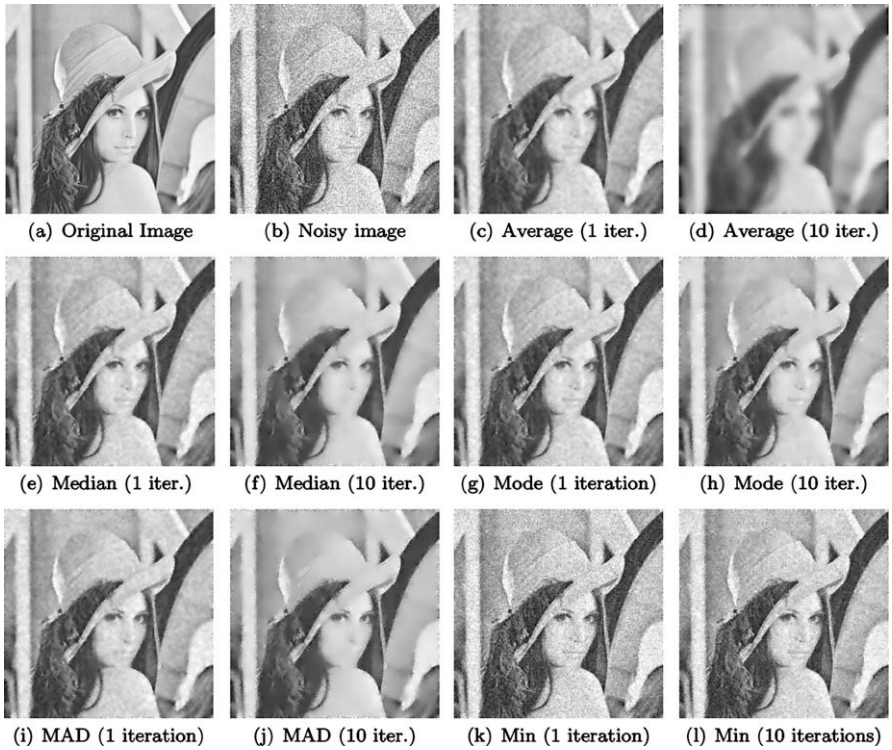

Fig. 15. Wiener and iterative Wiener filtering (10 iterations) of and image corrupted with additive Gaussian noise. Different noise estimators have been used. ($\sigma_n = 25$).

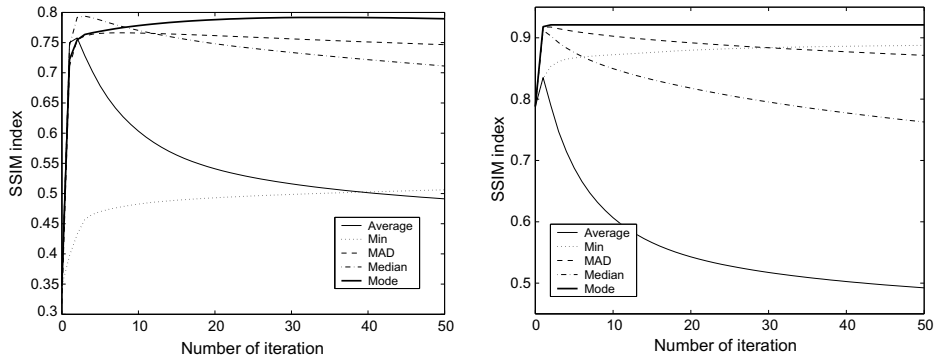

Fig. 16. SSIM quality index for a recursive Wiener filtering. Noise estimation using average, median, mode, MAD and minimum.

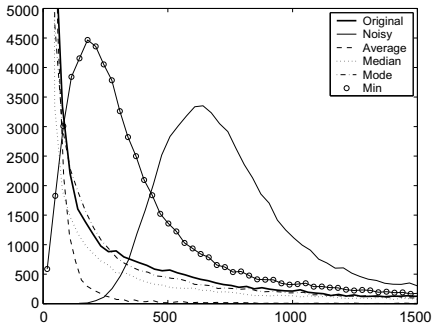

Fig. 17. Local variance distribution of Lenna with additive noise. Original image (bold) and noisy image (continuous) vs. Wiener filtered with different estimators: Average, median, mode and minumum. 10 iterations are considered. ($\sigma_n = 25$).

example. Consider the two textured images in Figs. 20a and 20b with gray levels in [0,255]. We have added Gaussian noise with zero mean and variance $\sigma_n = 75$. Noisy images are shown in Figs. 20c and 20d. Figs. 21 and 22 show the distribution of local variance (estimated by means of a 7×7 window) of the original and noisy images respectively. The modes of these distributions are:

Mode	Original	Noisy
Texture 1	2000	7500
Texture 2	9	6200

Clearly, in the first case the mode overestimates the value of noise; this is due to the non-null value of the mode of the original histogram. As for the second case, since the original histogram happened to have the mode located nearby the value 0, the mode of the noisy image is in the vicinity of real noise power.

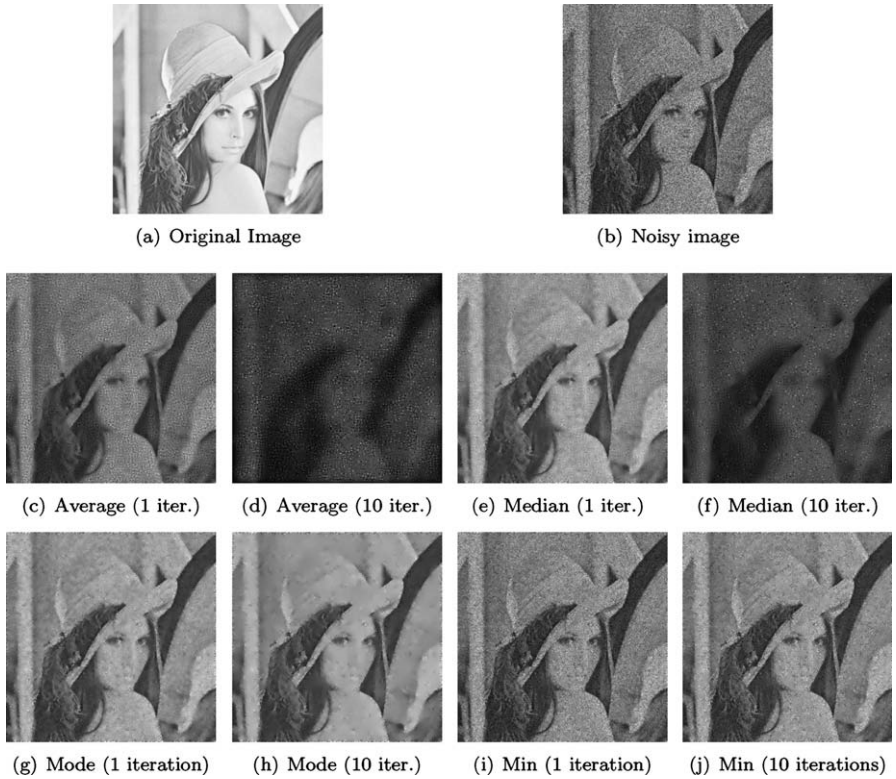

Fig. 18. Lee and iterative Lee filtering (10 iterations) of and image corrupted with multiplicative Gaussian noise. Different noise estimators have been used. ($C_u^2 = 0.036$).

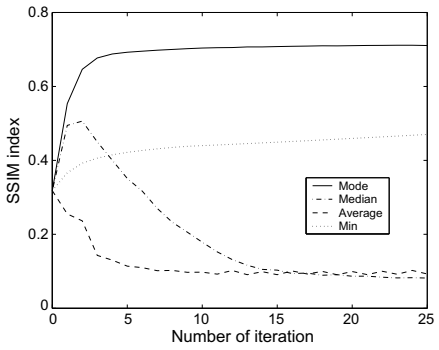

Fig. 19. SSIM quality index for a recursive Lee filtering. Noise estimation using average (dashed), median (dash-dotted), mode (continuous) and minimum (dotted).

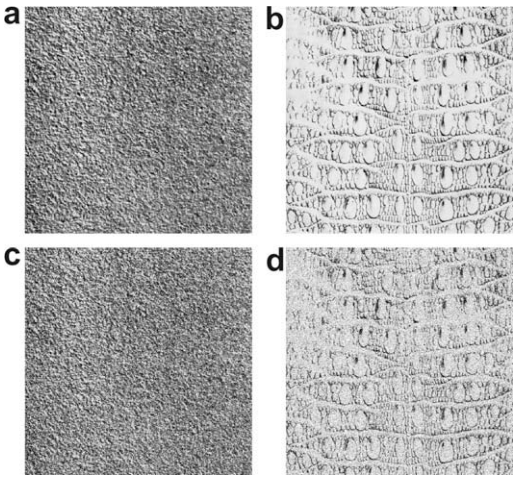

Fig. 20. Images of textures used in the experiments. (a) Texture 1. Original image. (b) Texture 2. Original image. (c) Texture 1 with additive noise ($\sigma = 75$). (d) Texture 2 with additive noise ($\sigma = 75$).

5. Concluding remarks

The main contribution of this paper is to show that a good and fast estimation of noise parameters can be obtained using the mode of the distribution of local sample statistics. Many real world images often encountered in practice have a great amount of uniform areas. Such images have a distribution of the local variance whose maximum value is around zero. When additive noise is added, this maximum is shifted to a value that corresponds to the variance of noise. The same effect may be observed with multiplicative noise and the coefficient of variation: the maximum of the local CV distribution is moved from zero to the actual value of the CV of noise. The variance of noise (if additive) can therefore be calculated using the mode of the sample variance distribution of the image. The same applies for multiplicative noise with the CV. This method presents some limitations when dealing with some textures, specially those with great variability.

Experiments show a better performance of the estimators proposed when compared with other simple estimation schemes. Accurate estimation of noise statistics is very important in recursive filtering, where noise becomes smaller in each iteration. Noise overestimation can affect to the stability of the process, as shown in the previous experiments. If some practical difficulties arise when calculating the mode out of a finite number of observations, the median may be used instead, with results fairly close to those of the mode; such a replacement is not advisable is small noise power is expected.

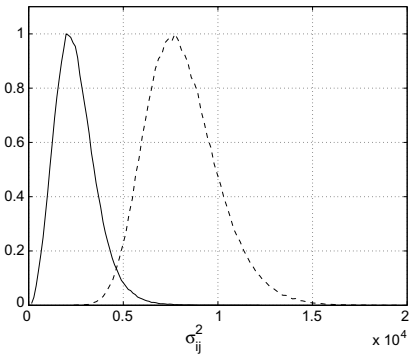

Fig. 21. (Normalized) Histogram of variances of texture 1: original image variances (solid) and noisy image (dashed).

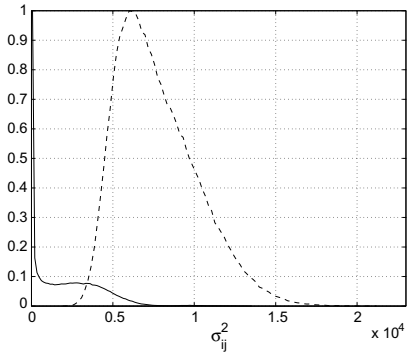

Fig. 22. (Normalized) Histogram of variances of texture 2: original image variances (solid) and noisy image (dashed).

Acknowledgments

The authors acknowledge the Comisión Interministerial de Ciencia y Tecnología for research Grant TEC2007-67073, the Fondo de Investigaciones Sanitarias for Grant PI-041483, Juna de Castilla y León for grants VA026A07, VA027A07, GRS 292/A/08 and the European Commission for the funds associated to the Network of Excellence SIMILAR (FP6-507609). The first author also acknowledges the MEC/Fulbright Commission for Grant FU2005-0716.

Appendix A. ML estimators

A.1. ML estimator for a Gaussian model

Let our data (the sampling variance) follow a Gamma distribution as defined in Section 3.1. We pursue to estimate the parameter σ^2. The likelihood function will be

$$p(\mathbf{x};\alpha,\beta) = \prod_i \gamma(x_i;\alpha,\beta) = \prod_i \frac{1}{\Gamma(\alpha)} x_i^{\alpha-1} \left(\frac{1}{\beta}\right)^{\alpha} \mathrm{e}^{-x_i/\beta} u(x_i)$$

and the log-likelihood

$$\log p(\mathbf{x};\alpha,\beta) = \sum_i \left[(\alpha-1)\log x_i - \alpha\log\beta - \frac{x_i}{\beta} - \log\Gamma(\alpha) \right] \quad \forall x_i > 0$$

If we take derivative with respect to β

$$\frac{\partial \log p(\mathbf{x};\alpha,\beta)}{\partial\beta} = \sum_i \left[-\frac{\alpha}{\beta} + \frac{x_i}{\beta^2} \right] = 0$$

from here

$$\hat{\beta} = \frac{1}{\alpha}\frac{1}{M}\sum_{i=1}^{M} x_i$$

being x_i the samples and M the number of samples. Using the relation $\sigma^2 = \beta\alpha$ and the invariance of the ML estimator we can write

$$(\hat{\sigma}^2)_{ML} = \frac{1}{M}\sum_{i=1}^{M} x_i$$

Note that in our case x_i are the samples of the local variance of the image.

A.2. ML estimator for the image plus noise model

Let our data (the sampling variance) follow the distribution defined in Section 3.2. We have an image with noise, whose local variance distribution can be modeled with $p_g(x)$, given by Eq. (25). To calculate the ML estimator for σ_n^2 we need the log-likelihood function, that can be defined as

$$\log p_g(\mathbf{x};\alpha_n,\beta_n,\beta_f) = \sum_i \left(-\log\Gamma(\alpha_n) + (\alpha_n-1)\log\beta_f - \alpha_n \times \log(\beta_f-\beta_n) - \frac{x_i}{\beta_f} + \log\gamma_l\left(\alpha_n, \left(\frac{1}{\beta_n}-\frac{1}{\beta_f}\right)x_i\right)\right)$$

We will find the estimator for β_n. We need to take derivative with respect to β_n and to β_f.

$$\begin{cases} \frac{\partial \log p_g(\mathbf{x};\alpha_n,\beta_n,\beta_f)}{\partial\beta_n} = \sum_i \left(\frac{\alpha_n}{\beta_f-\beta_n} + \frac{\frac{\partial\gamma_l()}{\partial\beta_n}}{\gamma_l()}\right) \\ \frac{\partial \log p_g(\mathbf{x};\alpha_n,\beta_n,\beta_f)}{\partial\beta_f} = \sum_i \left(\frac{\alpha_n-1}{\beta_f} - \frac{\alpha_n}{\beta_f-\beta_n} + \frac{x_i}{\beta_f^2} + \frac{\frac{\partial\gamma_l()}{\partial\beta_f}}{\gamma_l()}\right) \end{cases}$$

Let us calculate $\frac{\partial\gamma_l()}{\partial\beta_n}$ first. Applying the chain's rule

$$\frac{\partial}{\partial\beta_n}\gamma_l\left(\alpha_n,\left(\frac{1}{\beta_n}-\frac{1}{\beta_f}\right)x_i\right) = \frac{\partial\gamma_l(\alpha_n,\tau)}{\partial\tau}\frac{\partial\tau}{\partial\beta_n}$$

and

$$\frac{\partial\gamma_l(\alpha_n,\tau)}{\partial\tau} = \tau^{\alpha_n-1}e^{-\tau}$$

being $\tau = \left(\frac{1}{\beta_n}-\frac{1}{\beta_f}\right)x_i$. From this solution, we can write

$$\frac{\partial\gamma_l()}{\partial\beta_n} = \frac{\partial\gamma_l()}{\partial\tau}\frac{\partial\tau}{\partial\beta_n} = \left[\left(\frac{1}{\beta_n}-\frac{1}{\beta_f}\right)x_i\right]^{\alpha_n-1} e^{-\left(\frac{1}{\beta_n}-\frac{1}{\beta_f}\right)x_i}\left(\frac{-x_i}{\beta_n^2}\right) = -\frac{1}{\beta_n^2}F(x_i,\alpha_n,\beta_n,\beta_f)$$

being $F(x_i,\alpha_n,\beta_n,\beta_f) = \left[\left(\frac{1}{\beta_n}-\frac{1}{\beta_f}\right)x_i\right]^{\alpha_n-1} e^{-\left(\frac{1}{\beta_n}-\frac{1}{\beta_f}\right)x_i}x_i$. Then

$$\frac{\partial\log p_g(\mathbf{x};\alpha_n,\beta_n,\beta_f)}{\partial\beta_n} = \sum_i\left(\frac{\alpha_n}{\beta_f-\beta_n} - \frac{1}{\beta_n^2}\frac{F()}{\gamma_l()}\right)$$

And making it equal to 0 we have

$$\sum_i\left(\frac{\alpha_n}{\beta_f-\beta_n}\right) - \frac{1}{\beta_n^2}\sum_i\frac{F()}{\gamma_l()} = 0 \tag{34}$$

Let us calculate now the derivate with respect to β_f.

$$\frac{\partial}{\partial\beta_f}\gamma_l\left(\alpha_n,\left(\frac{1}{\beta_n}-\frac{1}{\beta_f}\right)x_i\right) == \frac{\partial\gamma_l(\alpha_n,\tau)}{\partial\tau}\frac{\partial\tau}{\partial\beta_f} = \left[\left(\frac{1}{\beta_n}-\frac{1}{\beta_f}\right)x_i\right]^{\alpha_n-1} e^{-\left(\frac{1}{\beta_n}-\frac{1}{\beta_f}\right)x_i}\left(\frac{x_i}{\beta_f^2}\right) = \frac{1}{\beta_f^2}F(x_i,\alpha_n,\beta_n,\beta_f)$$

and now

$$\frac{\partial\log p_g(\mathbf{x};\alpha_n,\beta_n,\beta_f)}{\partial\beta_f} = \sum_i\left(\frac{\alpha_n-1}{\beta_f} - \frac{\alpha_n}{\beta_f-\beta_n} + \frac{x_i}{\beta_f^2} + \frac{1}{\beta_f^2}\frac{F()}{\gamma_l()}\right)$$

And making it equal to 0 we have

$$\sum_i\frac{\alpha_n-1}{\beta_f} - \sum_i\frac{\alpha_n}{\beta_f-\beta_n} + \sum_i\frac{x_i}{\beta_f^2} + \sum_i\frac{1}{\beta_f^2}\frac{F()}{\gamma_l()} = 0 \tag{35}$$

From Eqs. (34) and (35) we can write

$$\sum_i\frac{\alpha_n-1}{\beta_f} - \sum_i\frac{\alpha_n}{\beta_f-\beta_n} + \sum_i\frac{x_i}{\beta_f^2} + \sum_i\frac{1}{\beta_f^2}\frac{\beta_n^2\alpha_n}{\beta_f-\beta_n} = 0$$

$$M\frac{\alpha_n-1}{\beta_f} - M\frac{\alpha_n}{\beta_f-\beta_n} + \sum_i\frac{x_i}{\beta_f^2} + M\frac{1}{\beta_f^2}\frac{\beta_n^2\alpha_n}{\beta_f-\beta_n} = 0$$

$$\beta_n = \frac{1}{\alpha_n}\frac{1}{M}\left(\sum_{i=1}^{M}x_i - M\beta_f\right)$$

and therefore

$$(\widehat{\sigma_n^2})_{ML} = \frac{1}{M}\sum_{i=1}^{M}x_i - \beta_f \tag{36}$$

being x_i the samples of the local variance of the noisy image. An estimator for β_f must be derived from function $F()$ and $\gamma_l()$.

Note than the same solution may have been obtained using the invariance property of the MLE [26], as the estimator of a sum of parameters is the sum of the MLE of each parameter:

$$(\widehat{\alpha_n\beta_n})_{ML} + (\widehat{\beta_f})_{ML} = \frac{1}{M}\sum_{i=1}^{M}x_i^n + \frac{1}{M}\sum_{i=1}^{M}x_i^f$$

being x_i^n the samples of the variance of noise and x_i^f the samples of the variance of the original image. As $x_i = x_i^n + x_i^f$

$$(\widehat{\sigma_n^2})_{ML} = \frac{1}{M}\sum_{i=1}^{M}x_i - (\widehat{\beta_f})_{ML}$$

Appendix B. Mode of the distribution in Eq. (25)

The purpose of this appendix is study the maximum of the distribution in Eq. (25) – rewritten here for convenience

$$p_g(x) = \frac{1}{\Gamma(\alpha_n)}\frac{\beta_f^{\alpha_n-1}}{(\beta_f-\beta_n)^{\alpha_n}}e^{-x/\beta_f}\gamma_l\left(\alpha_n,\left(\frac{1}{\beta_n}-\frac{1}{\beta_f}\right)x\right)u(x)$$

This distribution can be maximized by its derivative with respect x

$$\frac{\partial p_g(x)}{\partial x} = 0$$

$$K\left(\frac{-1}{\beta_f}\right)e^{-x/\beta_f}\gamma_l(\alpha_n,bx) + Ke^{-x/\beta_f}\frac{\partial\gamma_l(\alpha_n,bx)}{\partial x} = 0$$

$$\frac{\partial\gamma_l(\alpha_n,bx)}{\partial x} = \frac{1}{\beta_f}\gamma_l(\alpha_n,bx) \tag{37}$$

where $K = \frac{1}{\Gamma(\alpha_n)}\frac{\beta_f^{\alpha_n-1}}{(\beta_f-\beta_n)^{\alpha_n}}$ and $b = \left(\frac{1}{\beta_n}-\frac{1}{\beta_f}\right)$.

So, the mode of the distribution is the value of x that satisfies Eq. (37). Using integration by parts we know that [21]

$$\frac{\partial\gamma_l(\alpha_n,bx)}{\partial x} = b((\alpha_n-1)\gamma_l(\alpha_n-1,bx) - \gamma_l(\alpha_n,bx)) \tag{38}$$

So, replacing Eq. (38) into Eq. (37) we obtain this recurrence relation

$$\gamma_l(\alpha_n,bx) = \frac{b\beta_f}{1+b\beta_f}(\alpha_n-1)\gamma_l(\alpha_n-1,bx) \tag{39}$$

In order to solve the inversion problem, the lower incomplete gamma function can be represented as a confluent hypergeometric function [21]:

$$\gamma_l(\alpha_n,bx) = \frac{(bx)^{\alpha_n}}{\alpha_n}\cdot{}_1F_1(\alpha_n;\alpha_n+1;-bx)$$

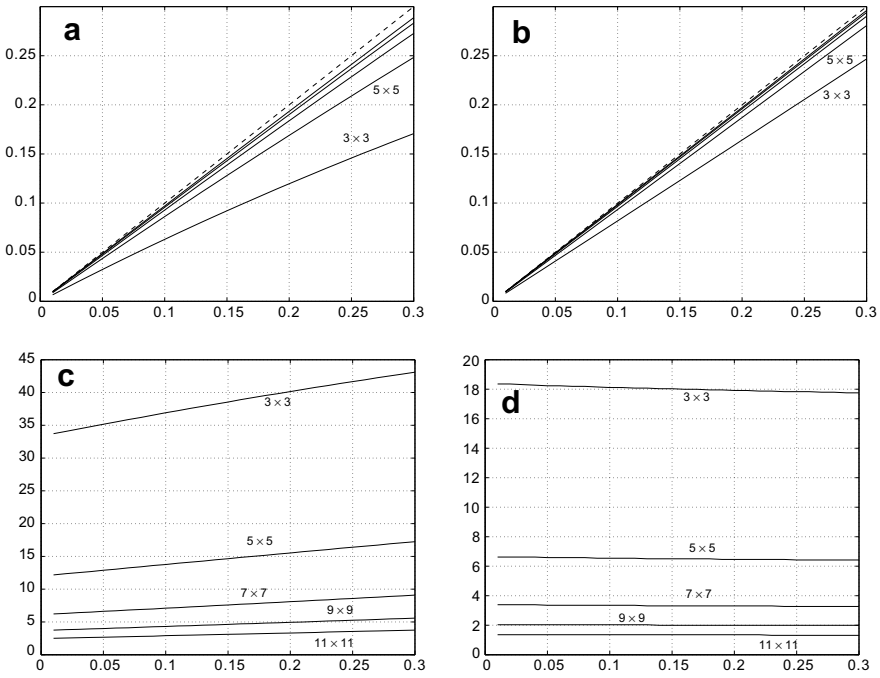

Fig. 23. Estimated CV using (a) the mode and (b) the median of pdf in Eq. (40). Estimated value (solid) vs. actual value (dashed line) as a function of the actual value. Samples sizes are 3×3 (labeled), 5×5 (labeled). Unlabeled curves are 7×7, 9×9 and 11×11, progressively approaching the dashed line. Relative estimation error using (c) the mode and (d) the median.

Fig. 24. Images to be analyzed. MRI from Brainweb [28]. Radiograph from Hospital Río Carrión, Palencia (Spain). Aerial picture from GOES Project Science (http://goes.gsfc.nasa.gov).

where ${}_1F_1(a;b;x)$ is confluent hypergeometric function of the first kind, defined

$${}_1F_1(\alpha_n;\alpha_n+1;-bx)=\sum_{k=0}^{\infty}\frac{\alpha_n}{\alpha_n+k}\frac{(-bx)^k}{k!}$$

When $bx\to 0$ it is clear that ${}_1F_1(\alpha_n;\alpha_n+1;-bx)\to 1$ and we can approximate

$$\gamma_l(\alpha_n,bx)\approx\frac{1}{\alpha_n}(bx)^{\alpha_n}$$

Note that when $bx\to 0$, β_f and β_n are approximately of the same order. From the point of view of our problem, that means that the variance of noise (proportional to β_n) and the distribution of variances in the image (modeled by β_f) are of the same magnitude. For large noise power values, the image tends to the pure Gaussian case. For very small values, the image cloaks the effect of the noise.

For this approximation, Eq. (39) becomes

$$\frac{1}{\alpha_n}(bx)^{\alpha_n}=\frac{b\beta_f}{1+b\beta_f}(bx)^{\alpha_n-1}$$

and therefore

$$x=\frac{\beta_f}{1+b\beta_f}\alpha_n=\frac{\beta_f}{1+\left(\frac{1}{\beta_n}-\frac{1}{\beta_f}\right)\beta_f}\alpha_n=\beta_n\alpha_n=\sigma_n^2$$

So, for this approximation

$$\arg\max_x p_g(x)=\sigma_n^2.$$

Appendix C. Sampling coefficient of variation

The case of the sampling CV is more involved. The reader is referred to [27] for details. Here we will only describe results. As before, consider $X_i, i=\{1,\dots,N\}$ are IID Gaussian random variables with non zero mean μ and standard deviation σ. Let $k^2=(\sigma/\mu)^2$ denote the actual (square) CV (we use the square magnitude to be consistent with the one used in the paper; in [27] the square is not used but results in our case are straightforward from the ones that the authors come up with). Let

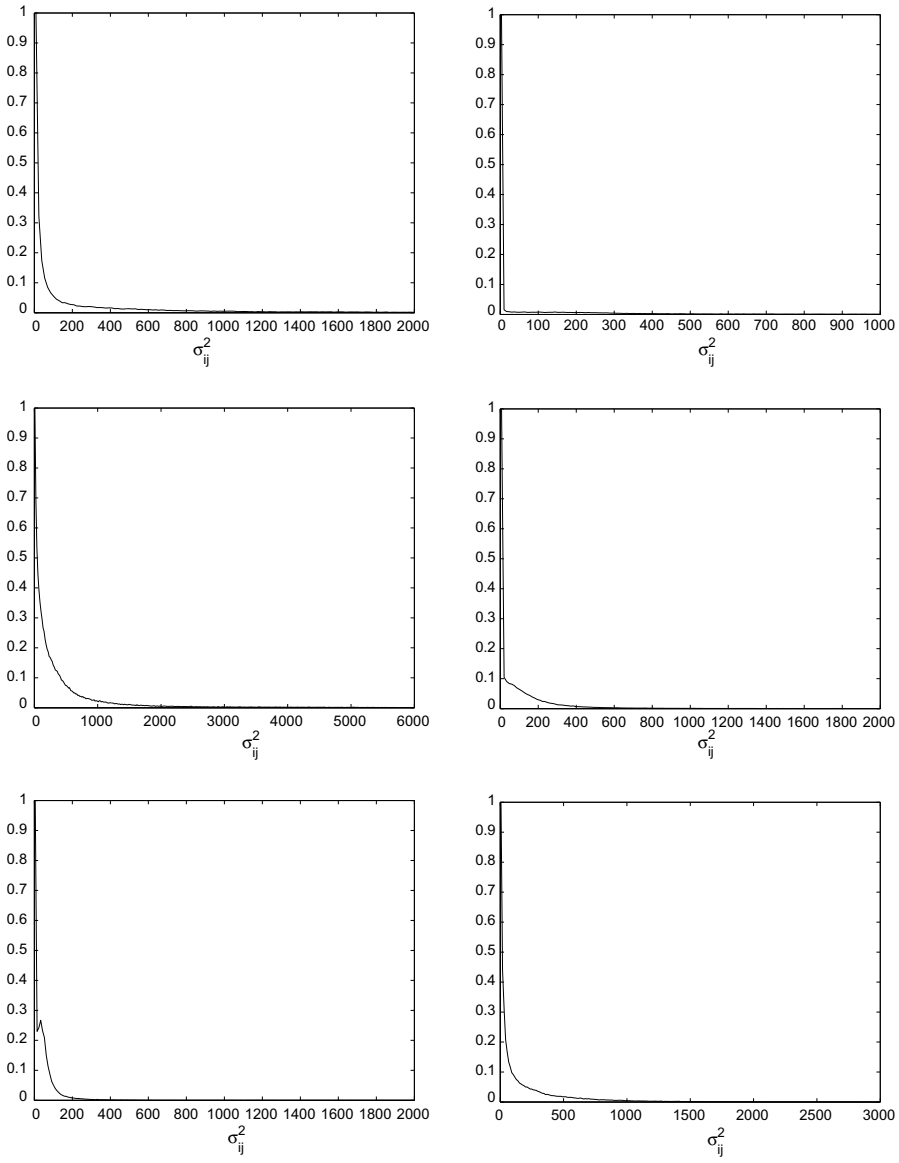

Fig. 25. Normalized distribution of local variances of the images in Fig. 24, displayed in the same order. A 5×5 window has been used.

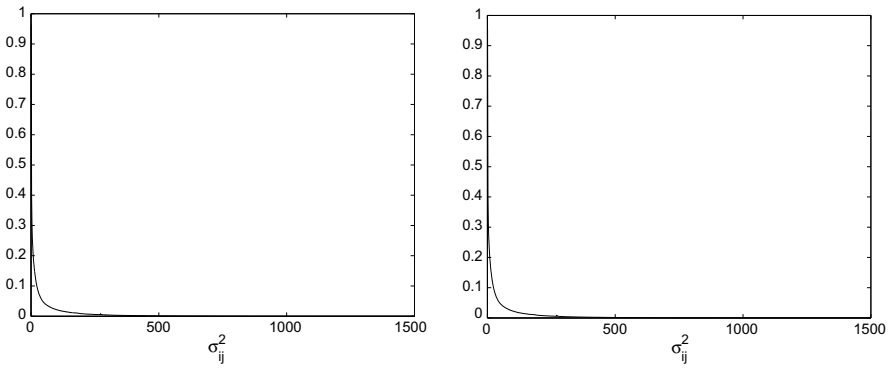

Fig. 26. Mean of the normalized distribution of local variances of the images from LIVE database [24]. A 5×5 window has been used. Gray scale images (left) and RGB images (right). Each color component have been evaluated separately.

$$C^2 = \frac{\frac{1}{N}\sum_{i=1}^{N}(X_i - \overline{X})^2}{\left(\frac{1}{N}\sum_{i=1}^{N} X_i\right)^2}.$$

Using lower case for actual values of C^2 and following [27] it is simple to obtain that the pdf of this variable is

$$f(c^2) = \begin{cases} \frac{1}{2c} g_N(c)[m_{N-1}(v_N(c)) - 2p_{N-1}(v_N(c))] & N \text{ odd} \\ -\frac{1}{2c} g_N(c) m_{N-1}(v_N(c)) & N \text{ even} \end{cases} \quad (40)$$

with

$$v_N(c) = \frac{\sqrt{N}}{k\sqrt{1+c^2}}$$

$$g_N(c) = \frac{2}{2^{(n-1)/2}\gamma_l\left(\frac{N-1}{2}\right)} \frac{c^{N-2}}{(1+c^2)^{N/2}} exp\left\{-\frac{N}{2k^2}\left(\frac{c^2}{1+c^2}\right)\right\}$$

and quantities $m_{N-1}(z)$ and $p_{N-1}(z)$ are the standard normal moment and the standard normal stop-loss moment of order $N-1$, respectively, about z. These moments can be obtained recursively, as follows

$$m_N(z) = (N-1)m_{N-2}(z) - zm_{N-1}(z), \quad n = 2, 3, \ldots$$

starting from

$$m_1(z) = -z, \quad m_0(z) = 1$$

With respect to the second set of moments we can write

$$p_N(z) = (N-1)p_{N-2}(z) - zp_{N-1}(z), \quad n = 2, 3, \ldots$$

starting from

$$p_1(z) = f(z) - z(1 - F(z)), \quad p_0(z) = 1 - F(z)$$

where $F(z)$ and $f(z)$ denote respectively the cumulative density function (cdf) and the pdf of a standard normal random variable.

As for the estimation, we have resorted to numerically finding both the mode and the median of the pdf in Eq. (40). Results are shown in Figs. 23(a) and 23(b) respectively for mode and median. Figures (c) and (d) show the relative error with respect to the actual value (for mode and median, respectively).

Appendix D. Local variance distribution in non-textured images

This paper is based on the assumption that the distribution of the local variances in a non-noisy image follows a distribution whose maximum is set on zero. To evaluate this assumption, the histogram of local variances of different kind of images has been evaluated. The images are shown in Fig. 24. Medical, meteorological and natural images have been used. The sampling local variance is calculated using 5×5 windows. The results are shown in Fig. 25. Finally, the mean of the distribution of 29 images from LIVE database [24] is presented in Fig. 26. Two cases have been considered: firstly, gray scale images and secondly RGB images where each color component have been evaluated separately.

References

[1] J.S. Lim, Two Dimensional Signal and Image Processing, Prentice Hall, Englewood Cliffs, NJ, 1990.
[2] J. Lee, Digital image enhancement and noise filtering using local statistics, IEEE Trans. Pattern Anal. Mach. Intell. 2 (2) (1980) 165–168.
[3] D.-H. Shin, R.-H. Park, S. Yang, J.-H. Jung, Noise estimation using adaptive Gaussian filtering, IEEE Trans. Consum. Electr. 51 (1) (2005) 218–226.
[4] D. Donoho, I. Johnstone, Ideal spatial adaptation by wavelet shrinkage, Biometrika 81 (1994) 425–455.
[5] J.-L. Starck, F. Murtagh, Automatic noise estimation from the multiresolution support, Publ. Astron. Soc. Pac. 110 (1998) 193–199.
[6] K. Konstantinides, B. Natarajan, G.S. Yovanof, Noise estimation and filtering using block-based singular value decomposition, IEEE Trans. Image Process. 6 (3) (1997) 479–483.
[7] M. Salmeri, A. Mencattini, E. Ricci, A. Salsano, Noise estimation in digital images using fuzzy processing, in: Proc. of the IEEE Int. Conf. on Image Processing, Thessaloniki (Greece), October 2001, pp. 517–520.
[8] Y. Yu, S. Acton, Edge detection in ultrasound imagery using the instantaneous coefficient of variation, IEEE Trans. Image Process. 13 (12) (2004) 1640–1655.
[9] M. Martín-Fernández, R. San-José-Estépar, C. Westin, C. Alberola-López, A novel Gauss-Markov random field approach for regularization of diffusion tensor maps, Lect. Notes Comput. Sci. 2809 (2003) 506–517.
[10] G. Gerig, O. Kbler, R. Kikinis, F. Jolesz, Nonlinear anisotropic filtering of MRI data, IEEE Trans. Med. Imaging 11 (2) (1992) 221–232.
[11] H.G. Hirsch, C. Ehrlicher, Noise estimation techniques for robust speech recognition, in: Proc. of the ICASSP, 1995, pp. 153–156.
[12] N.W.D. Evans, J.S. Mason, Noise estimation without explicit speech, non-speech detection: a comparison of mean, median and modal based approaches, in: Proc. Eurospeech, 2001, pp. 893–896.
[13] S. Aja-Fernández, C. Alberola-López, On the estimation of the coefficient of variation for anisotropic diffusion speckle filtering, IEEE Trans. Image Process. 15 (9) (2006) 2694–2701.
[14] D.T. Kuan, A.A. Sawchuk, T.C. Strand, P. Chavel, Adaptive noise smoothing filter for images with signal-dependent noise, IEEE Trans. Pattern Anal. Mach. Intell. 7 (2) (1985) 165–177.
[15] L. Kausmann, D. Kramer, L. Crooks, D. Ortendahl, Measuring signal-to-noise ratios in MR-imaging, Radiology 173 (1989) 265–267.
[16] R.D. Nowak, Wavelet-based rician noise removal for magnetic resonance imaging, IEEE Trans. Image Process. 8 (10) (1999) 1408–1419.
[17] P. Meer, J.-M. Jolion, A. Rosenfeld, A fast parallel algorithm for blind estimation of noise variance, IEEE Trans. Pattern Anal. Mach. Intell 12 (2) (1990) 216–223.
[18] N. Galatsanos, A.K. Katsaggelos, Methods for choosing the regularization parameter and estimating the noise variance in image restoration and their relation, IEEE Trans. Image Process. 1 (3) (1992) 322–336.
[19] A. Papoulis, Probability, Random Variables and Stochastic Processes, Mc-Graw Hill, New York, NY, 1991.
[20] A. Law, W.D. Kelton, Simulation, Modeling and Analysis, Mc-Graw Hill, New York, NY, 1991.
[21] M. Abramowitz, I.A. Stegun, Handbook of Mathematical Functions with Formulas, Graphs, and Mathematical Tables, ninth ed., Dover, New York, 1964.
[22] E. Parzen, On estimation of a probability density function and mode, Ann. Math. Stat. 33 (3) (1962) 065–1076.
[23] J. Venter, On estimation of the mode, Ann. Math. Stat. 38 (5) (1967) 1446–1455.

[24] Live Database, Laboratory for Image and Video Engineering (LIVE), The University of Texas, Austin [Online]. Available from: <http://live.ece.utexas.edu/research/quality/subjective.htm>.
[25] Z. Wang, A.C. Bovik, H.R. Sheikh, E.P. Simoncelli, Image quality assessment: from error visibility to structural similarity, IEEE Trans. Image Process. 13 (4) (2004) 600–612.
[26] S.M. Kay, Fundamentals of Statistical Signal Processing: Estimation Theory, Prentice Hall, New Jersey, 1993.
[27] W. Hürlimann, A uniform approximation to the sampling distribution of the coefficient of variation, Stat. Probabil. Lett. 24 (1995) 263–2689.
[28] BrainWeb, McConnell Brain Imaging Centre, Montreal Neurological Institute, McGill University [Online]. Available from: <http://www.bic.mni.mcgill.ca/brainweb/>.